COVER SHEET

NOTE: This coversheet is intended for you to list your article title and author(s) name only —this page will not appear in the book.

Title: Towards modelling of the frictional behaviour of deforming fibrous tows: A geometrical approach

Authors: Bo Cornelissen
Remko Akkerman

ABSTRACT

Fibrous tows used in continuous fibre-reinforced polymers (CFRPs) deform geometrically during the production of composite products. The cross-sectional geometry of the tow is influenced by the load-induced deformation mechanisms. A study of the effect of two commonly assumed geometrical tow shapes on an equivalent pressure distribution in a tow-on-a-pin spreading arrangement was performed. The preliminary results show that both elliptic and parabolic tow geometries have qualitatively the comparable equivalent pressure distributions.

INTRODUCTION

The mechanical properties of continuous fibre-reinforced polymers (CFRPs) or composite products are determined to a large extent during the forming phase. With any arbitrary production process of composite parts, the tool-surface-induced loads cause local cross-sectional changes in the tow. The fibre orientation and redistribution determine, to a large extent, the properties of a composite product. Therefore, knowledge of the tow orientation and tow deformation behaviour is essential to control the desired product quality in terms of mechanical performance, shape preservation and visual appearance.

The characterization of the process-generated friction mechanisms that occur when the tows are loaded is necessary to accurately predict the tow deformation in dry and impregnated fabrics as well as in individual tow or tape material.

A hierarchical modelling approach provides a framework for the description of the frictional behaviour of deforming fibrous tows. We define three scales to describe the constituents of CFRPs. The first and largest scale is the macro-scale: it represents the dimensions of plies and composite parts. Secondly, the dimensions of a typical fibrous tow are meso-scale related. Finally, the tow itself consists of several thousands of fibres which have dimensions on the micro-scale.

Bo Cornelissen and Remko Akkerman, University of Twente, Faculty of Mechanical Engineering, Chair of Production Technology, Horst Building room N128, P.O. Box 217, 7500 AE, Enschede, The Netherlands.

Generally, friction is treated as a dominant phenomenon in characterizing the forming phase of composite materials. The dominance of friction mechanisms at the macro-meso interaction level is acknowledged [1, 2], but at the meso-micro interaction level, it has been a less thoroughly studied phenomenon. This paper considers a model for the spreading of dry carbon fibre tows to assess the role of friction at the meso-micro interaction level. Besides the contribution of friction to the spreading of fibrous tows, a purely geometrical deformation of the tow is present. A comparison between predictions from a purely geometrical model of the spreading of fibrous tows and experimental data of spreading tows will provide an estimation of the contribution of friction to the observed deformation.

METHODOLOGY

Loading mechanisms involved in the deformation of fibrous tows

The study of meso-micro interactions is based on a break-down of an arbitrary process-induced load into more specific, simple loading mechanisms. This approach reflects the description of the macro-meso deformation mechanisms proposed by Long and Clifford [3]. The mechanisms act on both the meso and micro scales, thereby also affecting related mechanisms on the macro scale:

1. **tension**; the applied load acts in the axial direction with respect to the local tow or fibre axes
2. **compaction**; a compressive load acts perpendicularly to the longitudinal axes of the tows or fibres
3. **bending**; a moment is induced in a tow or fibre section; this results in flexure
4. **twist**; torsion – due to a relative rotation between two cross-sections along the fibre or tow axis – is applied along the longitudinal axes of the tows or fibres
5. **shear**; a load is induced by a relative displacement of two parallel planes, which remain parallel both during and after the displacement; the shear mechanism can be decomposed into a longitudinal and a transverse component, both with respect to the fibre axis.

This set of five distinct loading mechanisms describes the tow deformation behaviour during composite forming processes. However, this paper focuses on the role of the cross-sectional geometry of the tow in characterizing the tow deformation mechanisms. Other than pure tension, all the mechanisms stated above involve friction.

The role of friction depends on the type of load, the orientation of the tows or fibres and the type of friction interface. For example, in the case of bending, fibres in the tow slide along one another in the longitudinal direction, thereby causing a hysteretic effect [4]. Another example concerns the deformation of a set of two twisted yarns under a compressive load. The loads on the tow cause the migration of fibres, which involves friction both along and transverse to the fibre axis. Grishanov et al. described the modelling and simulation of this deformation case by using a minimal energy approach and a conformal mapping technique [5, 6].

The tow spreading model proposed by Wilson [7] gives an approach to calculate the width of a tow on a spreader bar, typically used in the production of pre-impregnated materials and filament winding. However, this approach implies a parabolic free surface shape. Other authors assumed an elliptic tow shape in their modelling approaches involving woven fabrics [8, 9]. A comparison between the normal force distribution for a parabolic tow cross-section and an elliptic cross-section based on Wilson's approach gives an indication of the relevance of the tow shape in the obtained normal force distribution.

This paper focuses on the prediction and evaluation of the normal force distribution for an elliptic as well as a parabolic cross-sectional tow shape.

Lateral tow spreading model

Wilson proposes a model for the lateral spreading of fibrous tows [7], a technique used in the production of pre-impregnated materials. Tows are pulled symmetrically over a spreader bar, which spreads the fibres laterally, thereby increasing the width and decreasing the thickness of the tow. Figure 1 shows a schematic description of half of the tow spreading arrangement. The width w of the spread tow takes the form:

$$w = (12AH)^{1/3} \tag{1}$$

where A is the cross-sectional area of the tow and H is the vertical displacement of the spreader bar. Wilson made five important assumptions in his model:

- uniform tension in the tow
- neglecting twist or entanglement effects
- a constant cross-sectional area of the tow (incompressibility)
- a continuum approach of the aggregate of the fibres in the tow
- neglecting any motion of fibres along their length.

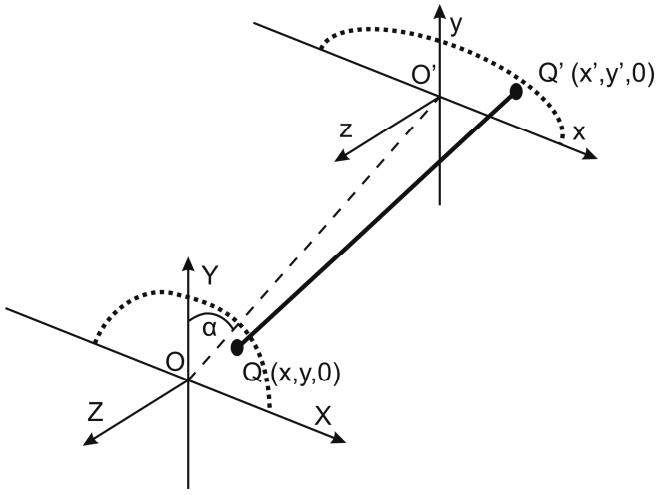

Figure 1: A flattening tow on a single circular spreader bar (located at O'x); half of the symmetrical arrangement is shown (symmetry plane xy). The tow is clamped in O and a tension T is applied at the ends. QQ' represents a typical fibre within the tow [7].

Wilson's experimental results supported his proposed theoretical approach. This implies that intra-tow friction does not play a major role in the spreading of fibrous tows. However, in those experiments polyamide and cotton tows were used rather than carbon fibres. Additionally, Wilson reports an error of 10-15% between theory and experiment, which he attributed to compressibility of the fibres, internal friction and possible fibre entanglements.

The predicted tow width from eq. (1) is derived from an assumed equivalent pressure distribution function of the cross-section of the tow. This pressure distribution, denoted by $p(x^*, y^*)$, is a parabolic function of the dimensionless width coordinate x^*, the dimensionless thickness coordinate y^* of the tow and the angle α, which defines the inclination of the tow with respect to the spreader bar (see Figure 1):

$$p = -\frac{1}{2}x^{*2} - y^* \cos(\alpha) + \frac{1}{2}\left(\frac{3}{2}\cos(\alpha)\right)^{2/3} \tag{2}$$

The author was able to calculate the shape of the tow on the spreader bar by deriving the free surface coordinates $y^*_s(x^*)$ from eq. (2), since the pressure at the free surface of the tow must be zero.

In this paper, the pressure distribution is calculated from a prescribed geometry. The calculation is based on the partial derivatives that lead to eq. (2) in [7]:

$$\frac{\partial p}{\partial x'} = \frac{2Tn}{L\ell}(x - x') \quad , \quad \frac{\partial p}{\partial y'} = \frac{2Tn}{L\ell}\left(-L\cos(\alpha) + (y - y')\sin^2(\alpha)\right). \tag{3}$$

Where T is the tension in the tow, n the number of fibres per unit cross-sectional area, ℓ the distance in longitudinal tow direction over which the tension acts (the contact width on the spreader bar) and L the length of the tow section between the initial tow cross-section locations (x, y) and the spread tow cross-section locations (x', y'). The pressure distribution $p(x', y')$ is found by integrating one of the partial derivatives of eq.(3), for example the derivative with respect to y':

$$p(y') = \int \frac{\partial p}{\partial y'} dy' \quad \rightarrow \quad p(y') = \frac{2Tn}{L\ell}\left(-L\cos(\alpha)\, y' + \left(yy' - \frac{1}{2}y'^2\right)\sin^2(\alpha) + C\right). \tag{4}$$

The integration constant can be a function of x', but it has to comply with the restriction set by the partial derivative of p with respect to x' in eq.(3). The derivative of the constant C – which is a function of x' – has to equal the partial derivative of p with respect to x' itself. Thus the following relation for $C(x')$ is obtained:

$$C'(x') = \frac{\partial p}{\partial x'} \quad \rightarrow \quad C(x') = \frac{2Tn}{L\ell}\left(xx' - \frac{1}{2}x'^2 + C_2\right), \tag{4}$$

$$p(x', y') = \frac{2Tn}{L\ell}\left(-L\cos(\alpha)\, y' + \left(yy' - \frac{1}{2}y'^2\right)\sin^2(\alpha) + xx' - \frac{1}{2}x'^2 + C_2\right). \tag{5}$$

In this case the integration constant C_2 cannot be a function of x', neither of y', as the requirements from eq.(3) would not be satisfied. However, one boundary condition regarding the free surface of the tow is not satisfied yet. The pressure at the free surface of the tow should equal zero (y_s (x_s) and y_s' (x_s') denote the free surface coordinates for the initial and deformed tow geometry, respectively). Hereby, the integration constant C_2 is defined:

$$p\left(x_s', y_s'\right) = 0 \rightarrow C_2 = L\cos\left(\alpha\right)\, y_s' - \left(y_s y_s' - \frac{1}{2} y_s'^2\right)\sin^2\left(\alpha\right) - x_s x_s' + \frac{1}{2} x_s'^2 \qquad (6)$$

The equation for the pressure distribution thus becomes:

$$p\left(x', y'\right) = \frac{2Tn}{L\ell}\left(\begin{array}{l} -L\cos\left(\alpha\right)\, y' + \left(y y' - \frac{1}{2} y'^2\right)\sin^2\left(\alpha\right) + x x' - \frac{1}{2} x'^2 + \\ L\cos\left(\alpha\right)\, y_s' - \left(y_s y_s' - \frac{1}{2} y_s'^2\right)\sin^2\left(\alpha\right) - x_s x_s' + \frac{1}{2} x_s'^2 \end{array}\right). \qquad (7)$$

The initial and deformed tow geometries are prescribed, for two different tow inclination angles α (Figure 1 shows the inclination angle): $0.01\,\pi$ (the tow is placed nearly vertically) and $0.49\,\pi$ (the tow is placed nearly horizontally) [rad]. Figure 2 shows the prescribed initial and deformed tow cross-sections for a parabolic and elliptic shape. The cross-sectional surface areas are constant for both shapes in the initial as well as the deformed state; the widths are prescribed, the tow thicknesses are determined by the constant area assumption and the prescribed width. The dimensions are normalized with respect to the parabolic tow geometry. Furthermore, the aforementioned assumptions made by Wilson also apply to this model.

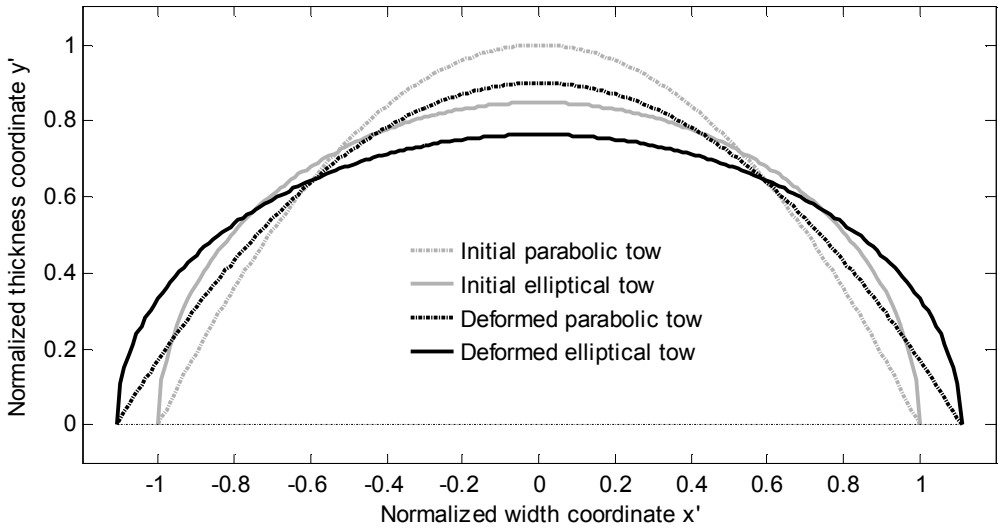

Figure 2: The free surface shapes of the parabolic and elliptic tow cross-sections; the surface areas remain constant, the coordinates are prescribed (10% flattened tows; equal widths).

RESULTS AND DISCUSSION

The plots in the next sections show the equivalent pressure distribution $p(x', y')$ for different tow inclination angles α. The prescribed tow geometries do not vary with α, the result of this approach is discussed in the 'Discussion of the results' section.
Table 1 shows the input variables of the model. The rather unusual values were used for ease of calculation and have a preliminary character.

TABLE 1: INPUT VARIABLES OF THE EQUIVALENT PRESSURE DISTRIBUTION MODEL

Variable	Value	Variable	Value
Tension T	1 $[N]$	Initial tow width	1 $[m]$
Number of fibres n	1 $[1/m^2]$	Deformed tow width	1.11 $[m]$
Pin contact length ℓ	$1 \cdot 10^{-3}$ $[m]$	Initial parabolic tow thickness	0.5 $[m]$
Tow length L	$1 \cdot 10^{-1}$ $[m]$	Final parabolic tow thickness	0.45 $[m]$
Cross-sectional surface	2/3 $[m^2]$	Inclination angle α	0.01; 0.49 π $[rad]$

Pressure distributions for the parabolic tow cross-section

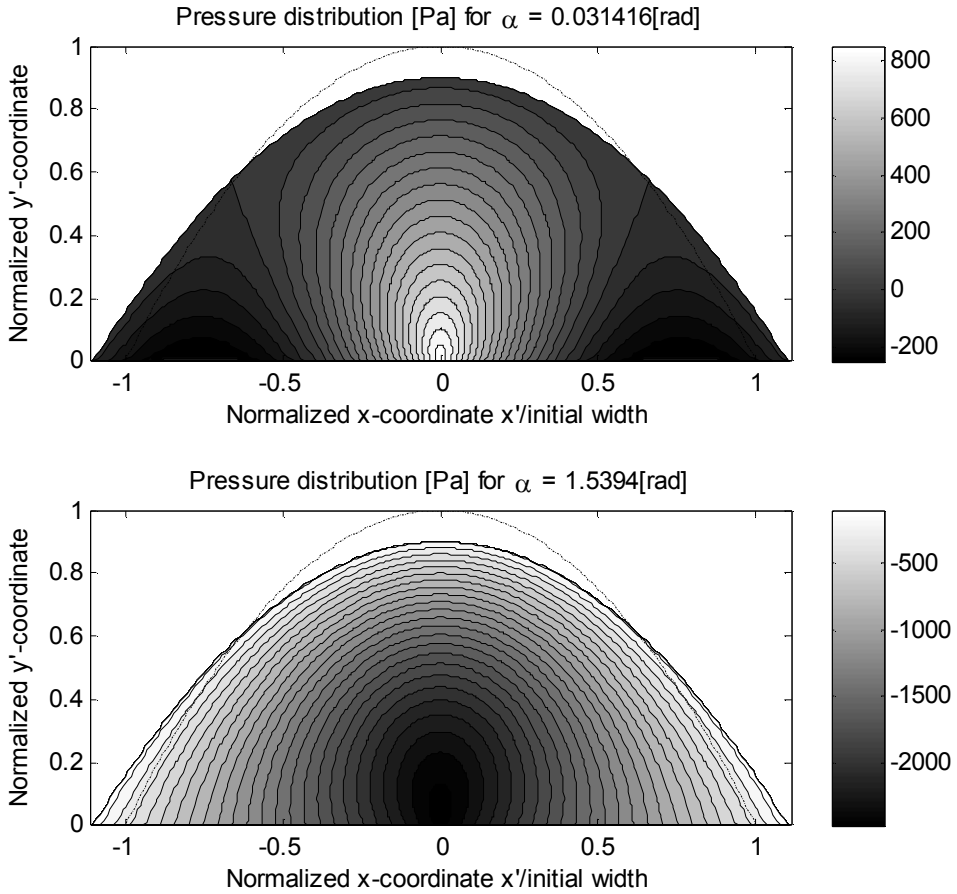

Figure 3: The equivalent pressure distribution $p(x', y')$ for a parabolic tow cross-section for the two extreme values of the tow inclination angle α.

Pressure distributions for the elliptic tow cross-section

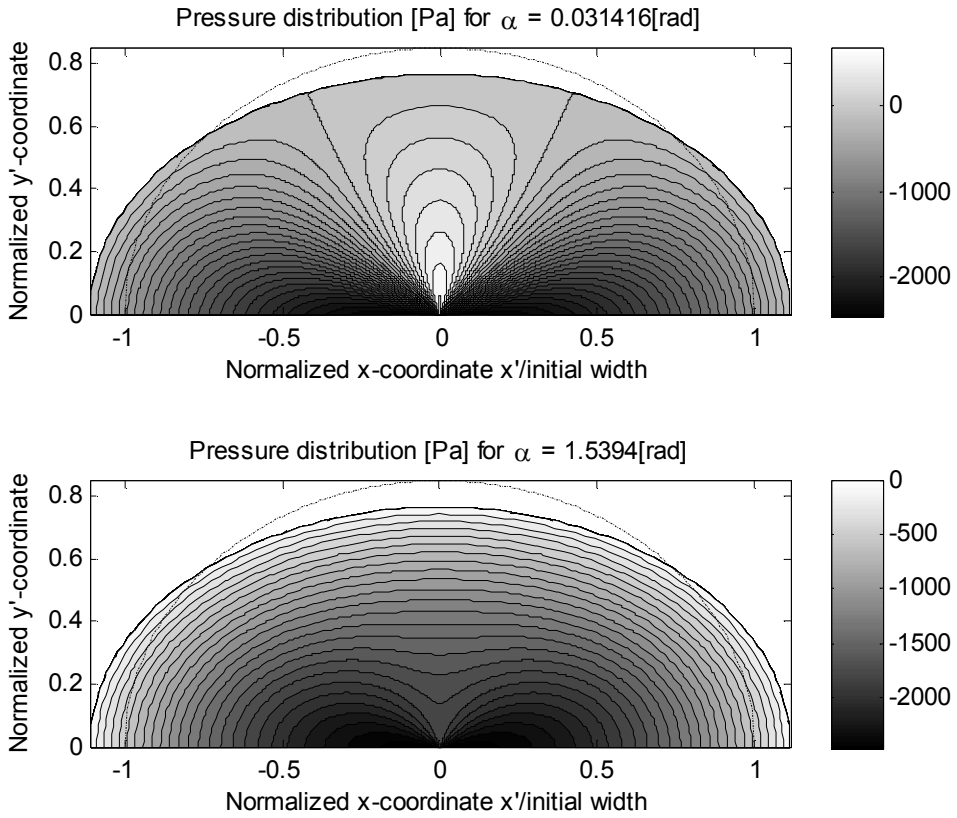

Figure 4: The equivalent pressure distributions $p(x', y')$ for an elliptic tow cross-section for the two extreme values of the tow inclination angle α.

Discussion of the results

The influence of the inclination angle α on the equivalent pressure distribution is clearly visible in the distribution plots of figures 3 and 4. The Plots show a sign change of the pressure for $\alpha=0.01\pi$ [rad] (this corresponds to an almost vertical tow arrangement). This suggests that the prescribed tow geometry and the prescribed boundary condition (the pressure is zero at the free surface of the tow) in combination with a chosen α-value overdetermine the pressure calculation. This results in a physically unexpected pressure distribution. The strong influence of α on the pressure distribution supports Wilson's theory [7] that the normal force distribution and thereby the spreading of a tow is governed by the inclination of the tow on the pin.

Integration of the pressure over the pin contact area should give the normal force exerted by the inclined tow on the pin:

$$N = \int_{-x'}^{x'} p(x,0)dx \tag{8}$$

At the moment of writing, the variation of the prescribed tow geometry with α was not yet implemented, as well as the normal force calculation of eq.(8).

CONCLUSION

An equivalent pressure approach was used to calculate the normal force distributions in single tows with a parabolic and elliptic cross-sectional shape on a spreader bar. The aim of the modelling approach was to assess the role of the cross-sectional shape of a single tow which is loaded by a normal force, induced by tension in the tow.

The results showed that the equivalent pressure distribution is comparable for both elliptic and parabolic tow cross-sectional shapes. However, no quantitative conclusions are drawn from the presented preliminary results, based on the two prescribed geometries and the obtained equivalent pressure distributions.

The angle of incidence of the tow with respect to the spreader bar plays a large role in the force distribution and the shape of the tow. A sign change in the predicted equivalent pressure distribution in the tow cross-section for certain inclination angles is caused by the fixed prescribed tow deformation. The geometry of both the elliptic and parabolic tows should vary with the inclination angle of the tow α.

Experimental validation of the normal force distribution with for example a pressure-foil on a pin will give better insight in the physical meaning of the model.

In this paper, the spreading of a tow on a pin used in impregnation processes was taken as a practical application of geometrical deformation of single tows in contact with a small surface. However, in most applications, the tows are organised in a woven structure. Therefore, it is interesting to apply the approach in a modified form on a tow configuration seen in woven structures.

REFERENCES

1. Lomov, S.V., A.V. Gusakov, G. Huysmans, A. Prodromou and I. Verpoest. 2000. "Textile geometry preprocessor for meso-mechanical models of woven composites,"*Compos. Sci. Technol.*, 60(11): 2083-2.
2. ten Thije, R.H.W. and R. Akkerman. 2009 "A multi-layer triangular membrane finite element for the forming simulation of laminated composites," *Compos. Part A Appl. Sci. Manuf.*, 40(6-7):739-753.
3. Long, A.C. and M.J. Clifford. 2007. "Composites forming mechanisms and materials characterization," in *Composites forming technologies,* A.C. Long, ed. Cambridge: Woodhead Publishing, pp. 1-21.
4. Lahey, T. and G. Heppler. 2004. "Mechanical modeling of fabrics in bending," *J. Appl. Mech. Trans. ASME,* 71(1): 32-40.
5. Grishanov, S.A., S.V. Lomov, R.J. Harwood, T. Cassidy and C. Farrer. 1997. "The simulation of the geometry of two-component yarns. Part I: The mechanics of strand compression: Simulating yarn cross-section shape," *J. Text. Inst. Part 1, Textile Inst.*, 88(2):118-131.
6. Grishanov, S.A., S.V. Lomov, T. Cassidy and R.J. Harwood. 1997. "The Simulation of the Geometry of a Two-component Yarn Part II: Fibre Distribution in the Yarn Cross-section," *J. Text. Inst.*, 88(4): 352-367.
7. Wilson, S.D.R. 1997. "Lateral spreading of fibre tows," *J. Eng. Math.*, 32(1):19-26.
8. Liu, L., Chen, J., Gorczyca, J., Sherwood, J. 2004. "Modeling of friction and shear in thermostamping of composites - Part II," *J. Compos. Mater.*, 38(1):1931-1947.
9. Chang, S., Sutcliffe, M.P.F. and Sharma, S.B. 2004. "Microscopic investigation of tow geometry changes in a woven prepreg material during draping and consolidation," *Compos. Sci. Technol.*, 64(1):1701-1707.